

Strange hidden-charm $P_{\psi_s}^\Lambda(4459)$ and $P_{\psi_s}^\Lambda(4338)$ pentaquarks and additional $P_{\psi_s}^\Lambda$, $P_{\psi_s}^\Sigma$ and $P_{\psi_{ss}}^N$ candidates in a quark model approach

Pablo G. Ortega,^{1,2,*} David R. Entem,^{2,3,†} and Francisco Fernández^{2,3,‡}

¹*Departamento de Física Fundamental,*

Universidad de Salamanca, E-37008 Salamanca, Spain

²*Instituto Universitario de Física Fundamental y Matemáticas (IUFFyM),*

Universidad de Salamanca, E-37008 Salamanca, Spain

³*Grupo de Física Nuclear, Universidad de Salamanca,*

E-37008 Salamanca, Spain

(Dated: February 1, 2023)

Hidden-charm pentaquark-like $P_{\psi_s}^\Lambda(4459)^0$ and $P_{\psi_s}^\Lambda(4338)$ resonances are studied in a constituent quark model as molecular meson-baryon structures. Such states are found in the $J^P(I) = \frac{1}{2}^-(0)$ channel with masses and widths compatible with the experimental measurements in a coupled-channels calculation with all the parameters constrained from previous studies. Other candidates are explored in the $J^P = \frac{1}{2}^-, \frac{3}{2}^-$ and $\frac{5}{2}^-$ channels in the charm and bottom sectors, with isospins 0 ($P_{\psi_s}^\Lambda$ and $P_{\Upsilon_s}^\Lambda$) and 1 ($P_{\psi_s}^\Sigma$ and $P_{\Upsilon_s}^\Sigma$). Additionally, the formalism is extended to study the $P_{\psi_{ss}}^N$ ($P_{\Upsilon_{ss}}^N$) pentaquarks, where eight candidates are predicted as $\bar{D}_s \Xi_c$ molecules in $I = \frac{1}{2}$, with $J^P = \frac{1}{2}^-, \frac{3}{2}^-$ and $\frac{5}{2}^-$ for the charm sector and nine candidates as $B_s \Xi_b$ for the bottom one.

Keywords: Quark model, Charmed baryon, Baryon-meson molecules, Hidden-charm pentaquarks, Hidden-bottom pentaquarks

I. INTRODUCTION

The discovery of pentaquark states by the LHCb [1] revolutionized Hadron Physics, expanding the usual qqq structure to four quarks and an antiquark. The first observations detected in the $J/\psi p$ mass spectrum showed two resonances, dubbed $P_c(4380)^+$ and $P_c(4450)^+$, close to $D^{(*)}N$ thresholds, which suggested a baryon-meson molecular nature in contrast to a compact pentaquark core. A further analysis showed that the higher resonance actually consisted in two separated narrow states, the $P_c(4440)^+$ and $P_c(4457)^+$, whereas a new state $P_c(4312)^+$ was detected [2].

The detection of such pentaquarks, with minimum $\bar{c}uud$ quark content, encouraged many authors [3–6] to predict similar hidden-charm structures with strangeness, i.e. with $\bar{c}cuds$, whose existence were recently confirmed with the discovery of the so-called $P_{cs}(4459)^0$ [7].

The $P_{\psi_s}^\Lambda(4459)^0$, following the nomenclature for exotic states proposed by LHCb Collaboration [8], was first spotted in the $J/\psi \Lambda$ invariant mass distribution from an analysis of the $\Xi_b^- \rightarrow J/\psi \Lambda K^-$ decays [7] with a 3σ significance. The state is an isospin-0 pentaquark-like resonance with a $\bar{c}cuds$ minimum quark content. The mass and width of this exotic state were measured to be

$$\begin{aligned} M_{P_{\psi_s}^\Lambda(4459)^0} &= 4458.8 \pm 2.9_{-1.1}^{+4.7} \text{ MeV}/c^2, \\ \Gamma_{P_{\psi_s}^\Lambda(4459)^0} &= 17.3 \pm 6.5_{-5.7}^{+8.0} \text{ MeV} \end{aligned} \quad (1)$$

that is, just 19 MeV below the $\bar{D}^{*0} \Xi_c^0$.

Since its discovery, there has been a plethora of studies trying to unveil the nature of such resonance, among which the most popular explanation is the meson-baryon molecular structure [9–23]. The J^P of the resonance was not experimentally determined due to a limited signal yield, but most studies favour a $J = \frac{1}{2}$ and/or $\frac{3}{2}$ with negative parity, which would allow the closest meson-baryon thresholds to be in a relative S-wave. Some studies (see e.g. Ref. [6]), predicts two $J^P = \frac{1}{2}^-$ and $J^P = \frac{3}{2}^-$ resonances close in mass, which can be unresolved in the original $P_{\psi_s}^\Lambda(4459)$ signal. The LHCb analyzed this two-resonance hypothesis, but could not confirm nor refute it.

Recently [24], the LHCb has announced another $P_{\psi_s}^\Lambda$ in the $J^P = \frac{1}{2}^-$ sector in the $B^- \rightarrow J/\psi \Lambda \bar{p}$ reaction, close to the $\bar{D}^- \Xi_c^+$ threshold in S-wave with isospin 0, denoted $P_{\psi_s}^\Lambda(4338)$, with mass and width:

$$\begin{aligned} M_{P_{\psi_s}^\Lambda(4338)^0} &= 4338.2 \pm 0.7 \pm 0.4 \text{ MeV}/c^2, \\ \Gamma_{P_{\psi_s}^\Lambda(4338)^0} &= 7.0 \pm 1.2 \pm 1.3 \text{ MeV} \end{aligned} \quad (2)$$

whose molecular nature has been explored in, e.g., Refs. [13, 25–27]. This new discovery points to a rich spectroscopy of pentaquark-like states in the hidden-charm sector, whose exploration has just started.

* pgortega@usal.es

† entem@usal.es

‡ fdz@usal.es

In this work, we will explore the hidden-charm strange pentaquark states $P_{\psi_s}^\Lambda$ as $\bar{D}^{(*)}\Xi_c^{(\prime)(*)}$ molecular states, and their bottom partners, in a coupled-channels formalism, using a constituent quark model which has been extensively used to describe meson and baryon spectrum [28–30] and, in particular, exotic states in the baryon spectrum as meson-baryon molecules [31–33].

The paper is organized as follows: In Section II we describe the details of the constituent quark model and the calculation of the resonances in a coupled-channels approach. In Sec. III we present the results and in Sec. IV we give a short summary.

II. THE MODEL

The QCD Lagrangian has a large global symmetry under $U(n_f) \times U(n_f)$ chiral rotations of n_f massless quark flavours. However, if chiral symmetry were conserved, we should see this symmetry in the hadron spectra. For example, chiral symmetry would imply the existence of a partner of opposite parity for each meson, which is clearly not the case in the experimental meson spectra. Current quark masses are non zero but have very small values that cannot explain the breaking in the spectra, therefore one can assume that chiral symmetry is spontaneously broken by the QCD vacuum. Then, due to Goldstone theorem, light pseudo-Goldstone bosons emerge, mediating the interaction among quarks. This phenomenology can be modeled using the instanton liquid mode of Ref. [34], which assumes that quarks interact with fermionic zero modes of individual instantons, acquiring a dynamical mass. A chiral invariant Lagrangian for quarks and Goldstone bosons which describes this effect is given by

$$\mathcal{L} = \bar{\psi}(i\gamma^\mu\partial_\mu - MU\gamma^5)\psi \quad (3)$$

where $U\gamma^5 = \exp(i\phi^a\lambda^a\gamma_5/f_\pi)$, ϕ^a denotes the pseudoscalar fields ($\vec{\pi}, K_i, \eta_8$) with $i = (1, \dots, 4)$, λ^a the $SU(3)$ flavor matrices and M the constituent quark mass. The constituent quark masses are momentum-dependent. Their dependence can be directly derived from the underlying theory, but a convenient parametrization can be used as $M(q^2) = m_q F(q^2)$, being $m_q \sim 300$ MeV and

$$F(q^2) = \sqrt{\frac{\Lambda_\chi^2}{\Lambda_\chi^2 + q^2}}, \quad (4)$$

where Λ_χ is a cut-off that controls the chiral symmetry-breaking scale.

Boson exchanges between light quarks show up when we expand the Goldstone boson field matrix $U\gamma^5$ from Eq. (3) as

$$U\gamma^5 = 1 + \frac{i}{f_\pi}\gamma_5\lambda^a\phi^a - \frac{1}{2f_\pi^2}\phi^a\phi^a + \dots \quad (5)$$

The first term can be identified with the constituent quark mass contribution, the second term with the one-boson exchange, that is π , K or η exchanges, whereas the main contribution of the third term can be modelled as a scalar σ exchange. Explicit expressions of the potentials derived from this expansion are detailed in Refs. [28, 35].

For the heavy quark sector, where the chiral symmetry is explicitly broken, the dynamics is not governed by Goldstone bosons but QCD perturbative effects. Those are considered through the one-gluon exchange term derived from the Lagrangian,

$$\mathcal{L}_{gqq} = i\sqrt{4\pi\alpha_s}\bar{\psi}\gamma_\mu G_c^\mu\lambda_c\psi, \quad (6)$$

where λ_c are the $SU(3)$ color generators and G_c^μ is the gluon field. The strong coupling constant α_s has a scale dependence which allows to consistently describe light, strange and heavy mesons, whose explicit expression is,

$$\alpha_s(\mu) = \frac{\alpha_0}{\ln\left(\frac{\mu^2 + \mu_0^2}{\Lambda_0^2}\right)} \quad (7)$$

where μ is the reduced mass of the $q\bar{q}$ system and α_0 , μ_0 and Λ_0 are parameters of the model.

The last piece is confinement, a QCD non-perturbative effect which excludes colored hadrons in nature. Within our CQM, this term is simulated by a linear-screened potential. In this picture, a quark-antiquark can be viewed as linked by a one-dimensional color flux-tube. At some scale, the spontaneous creation of a light $q\bar{q}$ pair can break the color flux-tube, which saturates the potential at the same interquark distance. The potential is, then,

$$V_{CON}(\vec{r}_{ij}) = \{-a_c(1 - e^{-\mu_c r_{ij}}) + \Delta\}(\vec{\lambda}_i^c \cdot \vec{\lambda}_j^c) \quad (8)$$

which behaves linearly at low r , with a strength given by $a_c\mu_c(\vec{\lambda}_i^c \cdot \vec{\lambda}_j^c)$, and a constant plateau at large r , given by $(\Delta - a_c)(\vec{\lambda}_i^c \cdot \vec{\lambda}_j^c)$

All the parameters of the model are constrained from previous studies on hadron phenomenology so, in this sense, the calculation is parameter free. This allows us to make robust predictions on the existence or nonexistence of specific molecular configurations. A first fit of the model parameters was done in Ref. [28], which analyzed the meson spectra from the aforementioned constituent quark model, previously used to study the NN phenomenology and baryons spectrum. An additional small update of the original parameters was, then, done in Ref. [35] from the study of $J^{PC} = 1^{--}$ charmonium spectroscopy.

The meson-baryon interaction emerges from the microscopic description at qq level using the Resonating Group Method (RGM). This way, we obtain an effective cluster-cluster interaction from the underlying quark-quark dynamics, where the wave functions of the meson and baryon act as natural cut-offs of the CQM potentials.

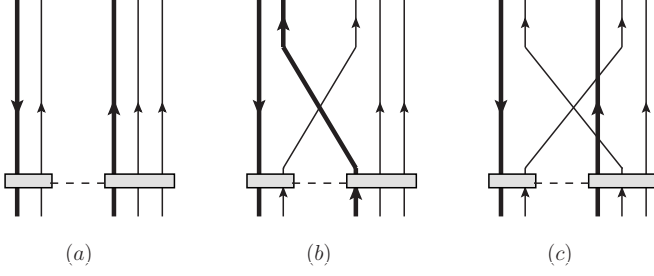


FIG. 1. Scheme of diagrams that are included in this work: Panel (a) are direct diagrams, including the $\{\sigma, \pi, \eta\}$ exchanges in the $\bar{D}^{(*)}\Xi_c^{(\prime)(*)} \rightarrow \bar{D}^{(*)}\Xi_c^{(\prime)(*)}$ channels, $\{\sigma, \eta\}$ in $\bar{D}_s^*\Lambda_c \rightarrow \bar{D}_s^*\Lambda_c$ reactions and the K exchange in $\bar{D}^{(*)}\Xi_c^{(\prime)(*)} \leftrightarrow \bar{D}_s^*\Lambda_c$ one. Panel (b) are diagrams with a $c \leftrightarrow n$ quark exchange between clusters, which describe the $\bar{D}^{(*)}\Xi_c^{(\prime)(*)} \leftrightarrow J/\psi(\eta_c)\Lambda$. Panel (c) are exchange diagrams which include a $n \leftrightarrow n$ exchange in $\bar{D}^{(*)}\Xi_c^{(\prime)(*)} \rightarrow \bar{D}^{(*)}\Xi_c^{(\prime)(*)}$ and $n \leftrightarrow s$ exchange in $\bar{D}^{(*)}\Xi_c^{(\prime)(*)} \leftrightarrow \bar{D}_s^*\Lambda_c$. The gray band represents the sum of interactions between quarks of different clusters, as detailed in the text (see Eqs. (9), (11) and (12)). The position of the charm quark is shown as a thick line.

For the system under consideration, as we have identical quarks between clusters, we have to take into account the full antisymmetric wave function of the $\bar{D}^{(*)}\Xi_c^{(\prime)(*)}$. We can separate the full antisymmetric operator of the 3-identical quark system, up to a normalization factor, as $\mathcal{A} = 1 - P_{12} - P_{13}$, where $P_{12}(P_{13})$ is the operator that exchanges the n quark from meson $\bar{D}^{(*)}$ (quark 1) and the second (third) n quark from baryon $\Xi_c^{(\prime)(*)}$. That is, a sum of interactions that includes direct potentials, with no quark rearrangement among clusters, and exchange potentials, which do allow quark shifts among them. These contributions are schematically shown in Fig. 1.

Then, the direct potentials can be written as

$$\begin{aligned} \text{RGM} V_D(\vec{P}', \vec{P}_i) &= \sum_{i \in M, j \in B} \int d\vec{p}_{M'} d\vec{p}_{B'} d\vec{p}_M d\vec{p}_B \times \\ &\times \phi_M^*(\vec{p}_{M'}) \phi_B^*(\vec{p}_{B'}) V_{ij}(\vec{P}', \vec{P}_i) \phi_{M'}(\vec{p}_M) \phi_{B'}(\vec{p}_B). \end{aligned} \quad (9)$$

with $\vec{P}^{(\prime)}$ the initial (final) relative momentum of the meson-baryon (MB) system, $\vec{p}_{M(B)}$ the relative internal momentum of the meson (baryon) and i (j) the indices that run inside the meson (baryon) constituents.

The exchange diagrams, on the contrary, have two effects. On the one side, they add self-interaction to the $\bar{D}^{(*)}\Xi_c^{(\prime)(*)}$ channels if light quarks are exchanged and, on the other side, they connect different channels otherwise disconnected, such as $\bar{D}^{(*)}\Xi_c$ and $J/\psi\Lambda$ channels.

For the first case, the exchange kernel $\text{RGM} K$ can be written as,

$$\text{RGM} K(\vec{P}', \vec{P}_i) = \text{RGM} H_E(\vec{P}', \vec{P}_i) - E_T \text{RGM} N_E(\vec{P}', \vec{P}_i), \quad (10)$$

which is a non-local and energy-dependent kernel that we split in a potential term plus a normalization term, being E_T the total energy of the system and \vec{P}_i a continuous parameter. Then, exchange Hamiltonian and normalization can be written as

$$\begin{aligned} \text{RGM} H_E(\vec{P}', \vec{P}_i) &= \int d\vec{p}_{M'} d\vec{p}_{B'} d\vec{p}_M d\vec{p}_B d\vec{P} \phi_{M'}^*(\vec{p}_{M'}) \times \\ &\times \phi_{B'}^*(\vec{p}_{B'}) \mathcal{H}(\vec{P}', \vec{P}) P_{mn} \left[\phi_M(\vec{p}_M) \phi_B(\vec{p}_B) \delta^{(3)}(\vec{P} - \vec{P}_i) \right], \\ \text{RGM} N_E(\vec{P}', \vec{P}_i) &= \int d\vec{p}_{M'} d\vec{p}_{B'} d\vec{p}_M d\vec{p}_B d\vec{P} \phi_{M'}^*(\vec{p}_{M'}) \times \\ &\times \phi_{B'}^*(\vec{p}_{B'}) P_{mn} \left[\phi_M(\vec{p}_M) \phi_B(\vec{p}_B) \delta^{(3)}(\vec{P} - \vec{P}_i) \right], \end{aligned} \quad (11)$$

where \mathcal{H} is the Hamiltonian at quark level and P_{mn} is the exchange operators P_{12} or P_{13} .

If we want to connect different channels, such as $\bar{D}^{(*)}\Xi_c$ and $J/\psi\Lambda$ channels, $\text{RGM} N_E$ does not affect and $\text{RGM} H_E$ can be reduced to an exchange potential,

$$\begin{aligned} \text{RGM} V_E(\vec{P}', \vec{P}_i) &= \sum_{i \in M, j \in B} \int d\vec{p}_{M'} d\vec{p}_{B'} d\vec{p}_M d\vec{p}_B d\vec{P} \phi_{M'}^*(\vec{p}_{M'}) \times \\ &\times \phi_B^*(\vec{p}_{B'}) V_{ij}(\vec{P}', \vec{P}) P_{mn} \left[\phi_{M'}(\vec{p}_M) \phi_{B'}(\vec{p}_B) \delta^{(3)}(\vec{P} - \vec{P}_i) \right]. \end{aligned} \quad (12)$$

In order to describe the meson $q\bar{q}$ and baryon qqq bound states, we solve the Schrödinger equation using the Gaussian Expansion Method [36]. In this method, the radial wave function of the cluster is expanded in terms of Gaussian functions whose parameters are in geometrical progression. For the radial meson wave function we can write

$$\phi_M^{\ell m}(\vec{p}) = \sum_n^{n_{\max}} C_n^{(M)} \phi_{n, \ell m}(\vec{p}) \quad (13)$$

where ℓ is the total angular momentum, m its projection and $C_n^{(M)}$ the coefficients of the base expansion. For the baryon, the radial wave function is similar, but we have two momenta for the ρ and λ modes,

$$\phi_B^{\ell m}(\vec{p}_\lambda, \vec{p}_\rho) = \sum_{n_\lambda, n_\rho}^{n_{\max}} C_{n_\lambda, n_\rho}^{(B)} \left[\phi_{n_\lambda, \ell_\lambda}(\vec{p}_\lambda) \phi_{n_\rho, \ell_\rho}(\vec{p}_\rho) \right]_{\ell m} \quad (14)$$

where $\ell = \ell_\lambda \oplus \ell_\rho$. In both cases, the ϕ functions are defined as

$$\phi_{n,\ell m}(\vec{p}) = N_{n\ell} p^\ell e^{-\frac{1}{4n}p^2} Y_{\ell m}(\hat{p}).$$

with $N_{n\ell}$ the normalization of the Gaussian wave functions such that $\langle \phi_{n\ell} | \phi_{n\ell} \rangle = 1$.

The coefficients C_n and the eigenenergies of the meson (baryon) are determined from the following set of equations,

$$\sum_{n=1}^{n_{\max}} \left[(T_{n'n} - EN_{n'n})C_n + \sum_{\alpha} V_{n'n} C_n \right] = 0 \quad (15)$$

with $T_{n'n}$ and $N_{n'n}$ the kinetic and normalization operators, which are diagonal, and $V_{n'n}$ the underlying qq interaction from the constituent quark model detailed above.

The masses and properties of meson-baryon molecular candidates are obtained from a coupled-channels calculation by searching the poles of the S -matrix, calculated by means of the T -matrix from the Lippmann-Schwinger equation

$$T_{\beta}^{\beta'}(z; p', p) = V_{\beta}^{\beta'}(p', p) + \sum_{\beta''} \int dp'' p''^2 V_{\beta''}^{\beta'}(p', p'') \frac{1}{z - E_{\beta''}(p'')} T_{\beta}^{\beta''}(z; p'', p) \quad (16)$$

where β represents the set of quantum numbers necessary to determine a partial wave in the meson-baryon state, $V_{\beta}^{\beta'}(p', p)$ is the RGM potential and $E_{\beta''}(p'')$ is the energy for the momentum p'' referred to the lower threshold. Eq. (16) is solved using a generalized version of the matrix inversion method [37] including channels with different thresholds, whereas poles are calculated by means of the Broyden method [38].

III. RESULTS

A. $P_{\psi_s}^{\Lambda}$ sector

The $P_{\psi_s}^{\Lambda}(4459)^0$ was first seen in the $J/\psi\Lambda$ invariant mass spectrum [7]. It is an isospin-0 resonance whose mass is between the $\bar{D}\Xi'_c$ and $\bar{D}^*\Xi_c$. Thus, it is reasonable to analyze its assignment as a $\bar{D}^{(*)}\Xi_c^{(\prime)}$ molecule. The most interesting sectors, which will be explored in this work, are $J^P = \frac{1}{2}^{-}$, $\frac{3}{2}^{-}$ and $\frac{5}{2}^{-}$, where the $\bar{D}^{(*)}$ and the $\Xi_c^{(\prime)(*)}$ are in a relative S-wave. States with positive parity are not favoured as it forces the molecule to be in a relative P-wave.

Hence, first we perform a coupled-channels calculation of $J^P = \frac{1}{2}^{-}$, $\frac{3}{2}^{-}$ and $\frac{5}{2}^{-}$ sectors including the channels detailed in Tab. I. The $J/\psi\Lambda$ and $\eta_c\Lambda$ channels have a

$P_{\psi_s}^{\Lambda}$		$P_{\psi_s}^{\Sigma}$		$P_{\Upsilon_s}^{\Lambda}$		$P_{\Upsilon_s}^{\Sigma}$	
Channel	Mass	Channel	Mass	Channel	Mass	Channel	Mass
$\eta_c\Lambda$	4099.1	$\eta_c\Sigma$	4176.5	$\eta_b\Lambda$	10514.7	$\eta_b\Sigma$	10592.1
$J/\psi\Lambda$	4212.6	$J/\psi\Sigma$	4290.0	$\Upsilon\Lambda$	10576.0	$\Upsilon\Sigma$	10653.4
$\bar{D}_s\Lambda_c$	4254.8	$\bar{D}_s\Sigma_c$	4421.9	$\bar{B}_s\Lambda_b$	10986.5	$\bar{B}_s\Sigma_b$	11180.3
$\bar{D}_s^*\Lambda_c$	4398.7	$\bar{D}_s^*\Sigma_c$	4565.7	$\bar{B}_s^*\Lambda_b$	11035.0	$\bar{B}_s^*\Sigma_b$	11228.8
$\bar{D}\Xi_c$	4336.6	$\bar{D}\Xi_c$	4336.6	$\bar{B}\Xi_b$	11072.7	$\bar{B}\Xi_b$	11072.7
$\bar{D}\Xi'_c$	4445.3	$\bar{D}\Xi'_c$	4445.3	$\bar{B}\Xi'_b$	11214.5	$\bar{B}\Xi'_b$	11214.5
$\bar{D}\Xi_c^*$	4513.2	$\bar{D}\Xi_c^*$	4513.2	$\bar{B}\Xi_b^*$	11233.3	$\bar{B}\Xi_b^*$	11233.3
$\bar{D}^*\Xi_c$	4477.9	$\bar{D}^*\Xi_c$	4477.9	$\bar{B}^*\Xi_b$	11117.9	$\bar{B}^*\Xi_b$	11117.9
$\bar{D}^*\Xi'_c$	4586.6	$\bar{D}^*\Xi'_c$	4586.6	$\bar{B}^*\Xi'_b$	11259.7	$\bar{B}^*\Xi'_b$	11259.7
$\bar{D}^*\Xi_c^*$	4654.5	$\bar{D}^*\Xi_c^*$	4654.5	$\bar{B}^*\Xi_b^*$	11278.5	$\bar{B}^*\Xi_b^*$	11278.5

TABLE I. Threshold masses (in MeV) of the meson-baryon channels considered in this work for the isospin-0 $P_{\psi_s}^{\Lambda}$ (minimum quark content $\bar{c}snn$), $P_{\Upsilon_s}^{\Lambda}$ ($\bar{b}bsnn$) and isospin-1 $P_{\psi_s}^{\Sigma}$ ($\bar{c}csnn$) and $P_{\Upsilon_s}^{\Sigma}$ ($\bar{b}bsnn$) states.

J^P	Assignment	Mass	Width
	$P_{\psi_s}^{\Lambda}(4338)$	4341.0	14.0
	$P_{\psi_s}^{\Lambda}(4459)$	4465.1	24.1
$\frac{1}{2}^{-}$	$P_{\psi_s}^{\Lambda}(4382)$	4381.7	76.7
	$P_{\psi_s}^{\Lambda}(4443)$	4443.6	0
	$P_{\psi_s}^{\Lambda}(4580)$	4581.0	7.4
	$P_{\psi_s}^{\Lambda}(4647)$	4647.5	2.7
$\frac{3}{2}^{-}$	$P_{\psi_s}^{\Lambda}(4655)$	4655.3	9.5

TABLE II. Masses and widths (in MeV) of the $P_{\psi_s}^{\Lambda}$ states found in this work. The resonances assigned to experimental states are shown in bold, the rest of states are theoretical predictions not yet detected.

small influence on the pole formation, but they contribute to the decay channels.

The states found in this calculation are shown in Tables II (masses and widths) and III (probabilities and partial widths). We find two resonances in the $J^P = \frac{1}{2}^{-}$ sector, with masses and widths compatible with the experimental $P_{\psi_s}^{\Lambda}(4459)^0$ and $P_{\psi_s}^{\Lambda}(4338)^0$. The theoretical $P_{\psi_s}^{\Lambda}(4459)^0$ resonance can be interpreted as a $\bar{D}^*\Xi_c$ molecule (59.5%) with a large admixture of $\bar{D}_s^*\Lambda_c$ (34.7%), which is its main decay channel. The $P_{\psi_s}^{\Lambda}(4338)^0$ candidate, on the contrary, is mainly a $\bar{D}_s\Lambda_c$ molecule (45%), due to the large coupling to this threshold, with a large admixture of $\bar{D}_s^*\Lambda_c$ (28%). This large admixture to the $\bar{D}_s\Lambda_c$ and $\bar{D}_s^*\Lambda_c$ for the $P_{\psi_s}^{\Lambda}(4459)^0$ and $P_{\psi_s}^{\Lambda}(4338)^0$ was also predicted at Ref. [6]. The predicted mass of the $P_{\psi_s}^{\Lambda}(4338)^0$ is in good agreement with the experimental value, just few MeV above it, due mainly to the inclusion of the $\bar{D}_s\Lambda_c$ threshold.

The partial widths are also shown in Table III. The

Assignment	Probabilities [%]										Partial widths [MeV]							
	$\eta_c\Lambda$	$J/\psi\Lambda$	$\bar{D}_s\Lambda_c$	$\bar{D}\Xi_c$	$\bar{D}_s^*\Lambda_c$	$\bar{D}\Xi'_c$	$\bar{D}^*\Xi_c$	$\bar{D}\Xi_c^*$	$\bar{D}^*\Xi'_c$	$\bar{D}^*\Xi_c^*$	$\eta_c\Lambda$	$J/\psi\Lambda$	$\bar{D}_s\Lambda_c$	$\bar{D}\Xi_c$	$\bar{D}_s^*\Lambda_c$	$\bar{D}\Xi'_c$	$\bar{D}\Xi_c^*$	$\bar{D}^*\Xi'_c$
$P_{\psi_s}^\Lambda(4338)$	7.3	4.4	45.0	6.3	28.0	0	9.0	0	0	0	1.2	0.6	11.0	1.1	0	0	0	0
$P_{\psi_s}^\Lambda(4459)$	0.9	0.2	1.3	3.4	34.7	0	59.5	0	0	0	0.7	1.6	3.4	1.9	16.6	0	0	0
$P_{\psi_s}^\Lambda(4382)$	3.5	2.2	10.7	5.6	55.8	0	22.2	0	0	0	2.1	30.8	43.2	0.7	0	0	0	0
$P_{\psi_s}^\Lambda(4443)$	0	0	0	0	0	99.5	0	0	0.4	0.1	0.1	0.9	0	0	0	0	0	0
$P_{\psi_s}^\Lambda(4580)$	0.2	0.6	0	0	0	20.6	0	0	78.3	0.3	0.1	0.1	0	0	0	7.2	0	0
$P_{\psi_s}^\Lambda(4647)$	0.0	0.0	0	0	0	18.0	0	0	9.0	73.0	0.004	0.002	0	0	0	2.0	0	0.6
$P_{\psi_s}^\Lambda(4655)$	0	0.0	0	0	0	4.8	0	25.2	22.3	47.8	0.01	0	0	0	0	0.3	6.1	3.1

TABLE III. Probabilities and partial widths of open-charmed channels in the $P_{\psi_s}^\Lambda$ states found in this work.

$P_{\psi_s}^\Lambda(4338)$ decays mainly to $\bar{D}_s\Lambda$, with also significant contributions to $\bar{D}\Xi_c$, $J/\psi\Lambda$ and $\eta_c\Lambda$. The width is, though, a bit larger than the experimental one, which could be explained by the large coupling to the $\bar{D}_s\Lambda_c$ channel. The $P_{\psi_s}^\Lambda(4459)$ has large partial widths to the $\bar{D}_s\Lambda$, $\bar{D}\Xi_c$ and $\bar{D}_s^*\Lambda_c$, which is its main decay channel. The $J/\psi\Lambda$ partial width is smaller, but relevant as it is the discovery channel. We want to remark that, as we employ a phenomenological model, systematic uncertainties cannot be evaluated, which should also be taken into account when comparing to experimental values.

Apart from the two experimentally confirmed states, $P_{\psi_s}^\Lambda(4338)$ and $P_{\psi_s}^\Lambda(4459)$, we find four additional $J^P = \frac{1}{2}^-$ and one $J^P = \frac{3}{2}^-$ $P_{\psi_s}^\Lambda$. The $J^P = \frac{3}{2}^-$ state, denoted as $P_{\psi_s}^\Lambda(4655)$, is a relatively narrow resonance around the $\bar{D}^*\Xi_c^*$ thresholds. It decays mostly to $\bar{D}\Xi_c^*$ and $\bar{D}^*\Xi'_c$. The $P_{\psi_s}^\Lambda(4382)$ is a wide $\frac{1}{2}^-$ resonance just below the $\bar{D}_s^*\Lambda_c$ ($\sim 56\%$), whose main decay channels are $J/\psi\Lambda$ and $\bar{D}_s\Lambda_c$. The so-called $P_{\psi_s}^\Lambda(4443)$, $P_{\psi_s}^\Lambda(4580)$ and $P_{\psi_s}^\Lambda(4647)$ are three $J^P = \frac{1}{2}^-$ molecules below the $\bar{D}\Xi'_c$, $\bar{D}^*\Xi'_c$ and $\bar{D}^*\Xi_c^*$ thresholds, respectively. They are relatively narrow, with widths below 10 MeV, which decay to the lower $\bar{D}\Xi'_c$ and $\bar{D}^*\Xi'_c$ channels. It is interesting to mention that, in our model, such resonances cannot decay to channels with a Λ_c or Ξ_c due to the different flavor structure of the baryon wave function. For such ground-state baryons, the flavor wave function of the light diquark is in an antisymmetric state, whereas for Ξ'_c and Ξ_c^* , the diquark is in a symmetric state, and the interaction between these structures is not allowed in our model.

B. $P_{\psi_s}^\Sigma$ sector

Additionally, we have explored the isospin 1 sector of the $\bar{c}snn$ system, i.e. the $P_{\psi_s}^\Sigma$ pentaquark states, with $J^P = \frac{1}{2}^-$, $\frac{3}{2}^-$ and $\frac{5}{2}^-$. The thresholds included in the coupled-channels calculation are mostly the same as for the isospin 0 calculation (see Table I). The pentaquark

J^P	Assignment	Mass	Width	$\Gamma_{J/\psi\Sigma}$	$\Gamma_{\bar{D}_s\Sigma_c}$	$\Gamma_{\bar{D}\Xi'_c}$	$\Gamma_{\bar{D}\Xi_c^*}$
$\frac{3}{2}^-$	$P_{\psi_s}^\Sigma(4547)$	4547.3	26.72	0.1	0.2	0	26.3
$\frac{5}{2}^-$	$P_{\psi_s}^\Sigma(4456)$	4456.8	74.57	0.01	47.9	26.6	0

TABLE IV. Masses, widths and partial widths (in MeV) of the $P_{\psi_s}^\Sigma$ states found in this work.

candidates found in this sector are shown in Tables IV (masses, widths and non-zero partial widths). Only two candidates are found just below the $\bar{D}^*\Xi_c^*$ threshold, a resonance in the $\frac{3}{2}^-$ channel close to $\bar{D}_s^*\Sigma_c$ threshold, with ~ 27 MeV width, and a wider resonance in $\frac{5}{2}^-$, above the $\bar{D}\Xi'_c$ thresholds. The partial widths show that $J/\psi\Sigma$ is a viable detection channels for the $\frac{3}{2}^-$ molecule, but open-charmed channels are more convenient to detect the $\frac{5}{2}^-$ resonance. In this case, channels with Ξ_c are disconnected from those containing a Σ_c , Ξ'_c or Ξ_c^* , due to the flavor symmetry of the light diquark in these baryons.

C. Hidden-bottom $P_{\Upsilon_s}^\Lambda$ and $P_{\Upsilon_s}^\Sigma$ sector

In this section we extend our analysis to the bottom sector, studying the hidden-bottom pentaquarks $P_{\Upsilon_s}^\Lambda$ and $P_{\Upsilon_s}^\Sigma$ states, with minimum quark content $\bar{b}bsnn$ and isospin 0 and 1, respectively. Our model allows to analyze such structures with no further tuning of the parameters. The reduction of the kinetic energy of the baryon-meson system due to the larger bottom quark mass favors the formation of new molecules, thus we find more candidates than for the charm sector.

We, then, explore the $\frac{1}{2}^-$, $\frac{3}{2}^-$ and $\frac{5}{2}^-$ sectors, including the channels of Table I, which are the bottom analogs of the coupled-channels calculation done for the $P_{\psi_s}^\Lambda$ and $P_{\psi_s}^\Sigma$ sectors. We obtain twelve $P_{\Upsilon_s}^\Lambda$ candidates and eleven $P_{\Upsilon_s}^\Sigma$ ones. Results are shown in Table V, detailing the sector, mass, total width and main decay channel. For most of them, $\Upsilon(1S)\Lambda$ is a good detection channel, in analogy with the $J/\psi\Lambda$ channel where the $P_{\psi_s}^\Lambda(4459)$ and $P_{\psi_s}^\Lambda(4338)$ pentaquarks were first detected.

	J^P	Mass	Width	Main Decay Channel
$P_{\Upsilon s}^\Lambda$		10671.8	89.2	$\Upsilon(1S)\Lambda$ (87.4)
		10994.8	5.2	$B_s\Lambda_b$ (3.6)
	$\frac{1}{2}^-$	11208.0	44.5	$B^*\Xi_c$ (33.1)
		11238.7	39.7	$B^*\Xi_b$ (19.2)
		11042.6	59.0	$B_s^*\Lambda_b$ (48.9)
		11098.5	83.6	$B_s\Lambda_b$ (64.6)
	$\frac{3}{2}^-$	11090.4	66.3	$B\Xi_b$ (56.8)
		11043.0	58.0	$B_s^*\Lambda_b$ (56.4)
		10995.9	57.7	$B_s\Lambda_b$ (54.9)
	$\frac{5}{2}^-$	11043.1	54.8	$B_s^*\Lambda_b$ (45.0)
	11098.6	47.1	$B\Xi_b$ (30.3)	
	11141.7	49.1	$B^*\Xi_b$ (29.8)	
$P_{\Upsilon s}^\Sigma$		11074.8	52.0	$B\Xi_b$ (52.0)
	$\frac{1}{2}^-$	11193.9	34.4	$B_s\Sigma_b$ (33.6)
		11132.4	66.2	$B^*\Xi_b$ (66.1)
	$\frac{3}{2}^-$	11188.1	59.1	$B_s\Sigma_b$ (58.8)
		11251.2	46.6	$B\Xi_b^*$ (23.9)
		11232.9	7.9	$B_s^*\Sigma_b$ (5.6)
	$\frac{5}{2}^-$	11079.9	54.4	$B\Xi_b$ (54.4)
		11125.2	52.9	$B^*\Xi_b$ (52.9)
		11193.2	41.5	$B_s\Sigma_b$ (41.4)
		11243.5	40.7	$B_s^*\Sigma_b$ (39.9)
	11272.5	30.5	$B_s^*\Sigma_b$ (17.4)	

TABLE V. Masses, widths and main decay channel, with partial width in parenthesis (in MeV), of the $P_{\Upsilon s}^\Lambda$ and $P_{\Upsilon s}^\Sigma$ states found in this work.

D. $P_{\psi ss}^N$ and $P_{\Upsilon ss}^N$ sectors

The $P_{\psi ss}^N$ ($P_{\Upsilon ss}^N$) are pentaquark-like states with $\bar{c}cssn$ ($\bar{b}bssn$) minimum quark content and $I = \frac{1}{2}$. Up to now, no states of this kind have been experimentally discovered. Yet, the similarity with the $P_{\psi s}^\Lambda$ states make them an interesting system that have been explored in the recent literature [27, 39–42], pointing to a rich spectroscopy. Our constituent quark model allows to make predictions of such states with no parameter tuning. The relevant thresholds for this system are given in Table VI.

In this sector, channels are mostly disconnected, as no π exchange is allowed between them and other diagrams such as annihilation through a gluon are negligible. Then, the dynamics is mostly governed by σ exchanges, which gives diagonal contributions. So, in this case, there is no gain in performing a coupled-channels calculation, and an analysis of individual thresholds can be considered as a good approach.

Results are shown in Table VII. In the hidden-charm sector we find eight $P_{\psi ss}^N$ meson-baryon molecules: three $\frac{1}{2}^-$, four $\frac{3}{2}^-$ and one $\frac{5}{2}^-$. Most of the candidates are potentially detectable in the $J/\psi\Xi$ or $\eta_c\Xi$ channels, the analogs of the $J/\psi\Lambda$ and $\eta_c\Lambda$ in the $P_{\psi ss}^N$ sector. For

$P_{\psi ss}^N$		$P_{\Upsilon ss}^N$	
Channel	Mass [MeV]	Channel	Mass [MeV]
$\bar{D}_s\Xi_c$	4437.72	$\bar{B}_s\Xi_b$	11160.08
$\bar{D}_s\Xi'_c$	4546.45	$\bar{B}_s\Xi'_b$	11301.90
$\bar{D}_s^*\Xi_c$	4581.57	$\bar{B}_s^*\Xi_b$	11208.60
$\bar{D}_s\Xi_c^*$	4614.27	$\bar{B}_s\Xi_b^*$	11320.70
$\bar{D}_s^*\Xi'_c$	4690.30	$\bar{B}_s^*\Xi'_b$	11350.42
$\bar{D}_s^*\Xi_c^*$	4758.12	$\bar{B}_s^*\Xi_b^*$	11369.21

TABLE VI. Masses of the meson-baryon channels considered in this work for the $P_{\psi ss}^N$ (minimum quark content $\bar{c}cssn$) and $P_{\Upsilon ss}^N$ (minimum quark content $\bar{b}bssn$).

	J^P	Channel	Mass [MeV]	Main Decay channels	
$P_{\psi ss}^N$	$\frac{1}{2}^-$	$\bar{D}_s\Xi_c$	4436.8	$J/\psi\Xi$ (9.9), $\eta_c\Xi$ (1.4)	
		$\bar{D}_s\Xi'_c$	4544.0	$J/\psi\Xi$ (1.0), $\eta_c\Xi$ (0.7)	
		$\bar{D}_s^*\Xi_c$	4580.8	$J/\psi\Xi$ (0.9), $\eta_c\Xi$ (1.0)	
	$\frac{3}{2}^-$	$\bar{D}_s^*\Xi_c$	4581.1	$J/\psi\Xi$ (1.2)	
		$\bar{D}_s\Xi_c^*$	4613.0	$J/\psi\Xi$ (0.8), $\eta_c\Xi^*$ (1.3)	
		$\bar{D}_s^*\Xi'_c$	4684.9	$\bar{D}_s^*\Xi_c^*$ (3.1), $J/\psi\Xi^*$ (7.7)	
			$\bar{D}_s^*\Xi_c^*$	4758.1	$\eta_c\Xi^*$ (0.03)
	$\frac{5}{2}^-$	$\bar{D}_s^*\Xi_c^*$	4751.7	$J/\psi\Xi^*$ (4.6)	
	$P_{\Upsilon ss}^N$	$\frac{1}{2}^-$	$B_s\Xi_b$	11142.6	$\Upsilon\Xi$ (1.3), $\eta_b\Xi$ (0.2)
			$B_s\Xi'_b$	11281.4	$\Upsilon\Xi^*$ (2.0)
$B_s^*\Xi'_b$			11348.5	$B_s\Xi'_b$ (22.4)	
			$B_s^*\Xi_b$	11191.9	$\Upsilon\Xi$ (0.2), $\eta_b\Xi$ (0.4)
			$B_s^*\Xi_b$	11194.2	$\Upsilon\Xi$ (0.3)
$\frac{3}{2}^-$		$B_s\Xi_b^*$	11304.0	$\Upsilon\Xi^*$ (0.5), $\eta_b\Xi^*$ (0.1)	
		$B_s^*\Xi'_b$	11321.8	$B_s^*\Xi_b^*$ (5.7), $\Upsilon\Xi^*$ (0.6)	
			$B_s^*\Xi_b$	11361.9	$B_s\Xi_c^*$ (0.4)
$\frac{5}{2}^-$		$B_s^*\Xi_b^*$	11337.6	$\Upsilon\Xi^*$ (0.5)	

TABLE VII. Predicted $P_{\psi ss}^N$ and $P_{\Upsilon ss}^N$ meson-baryon molecules. The main decay channels of each candidate is shown, with the partial width (in MeV) in parenthesis.

the hidden-bottom sector we find nine $P_{\Upsilon ss}^N$ molecules, with larger binding energies. The main decay channels for these candidates are mostly $\Upsilon\Xi^{(*)}$ and $\eta_b\Xi^{(*)}$.

IV. SUMMARY

In this work we have performed a coupled-channels calculation of the $P_{\psi s}^\Lambda$, $P_{\psi s}^\Sigma$ and $P_{\psi ss}^N$ hidden-charm pentaquark candidates, and their bottom partners $P_{\Upsilon s}^\Lambda$, $P_{\Upsilon s}^\Sigma$ and $P_{\Upsilon ss}^N$, as molecular states in the framework of a constituent quark model that satisfactorily describes the $P_{\psi s}^N$ states [32]. All the states presented in this work are predictions of the model, as all the parameters are constrained from previous studies.

We find that the $P_{\psi s}^\Lambda(4338)$ and $P_{\psi s}^\Lambda(4459)$ exper-

imental states can be described as $(I)J^P = (0)\frac{1}{2}^-$ baryon-meson molecules with minimum quark content $\bar{c}csnn$. Along with this experimental states, further $\bar{c}csnn$ molecules are predicted: four additional $\frac{1}{2}^-$ and one $\frac{3}{2}^- P_{\psi_s}^\Lambda$ molecules. Their properties (mass, width, probabilities and partial widths) are given, which could be useful for their experimental detection. Additionally, we have explored the isospin-1 partners, the $P_{\psi_s}^\Sigma$ pentaquarks, obtaining a narrow $\frac{3}{2}^-$ resonance and a wide $\frac{5}{2}^-$ one. For the bottom sector, $P_{\Upsilon_s}^\Lambda$ and $P_{\Upsilon_s}^\Sigma$, we obtain a rich spectroscopy, as a result of the reduction of the kinetic energy of the meson-baryon system due to the larger bottom quark mass.

In the $P_{\psi_{ss}}^N$ ($P_{\Upsilon_{ss}}^N$) sector, that is, structures with

isospin $\frac{1}{2}$ and minimum quark content $\bar{c}csn$ ($\bar{b}bsn$), we find up to eight molecular candidates as $\bar{D}_s^{(*)}\Xi_c^{(*)\prime}$ molecules and nine molecular candidates as $B_s^{(*)}\Xi_b^{(*)\prime}$ states, which can be detected in future LHCb searches.

ACKNOWLEDGMENTS

This work has been partially funded by Ministerio de Ciencia, Innovación y Universidades under Contract No. PID2019-105439GB-C22/AEI/10.13039/501100011033, and by the EU Horizon 2020 research and innovation program, STRONG-2020 project, under grant agreement No. 824093.

-
- [1] R. Aaij *et al.* (LHCb), Phys. Rev. Lett. **115**, 072001 (2015), arXiv:1507.03414 [hep-ex].
- [2] R. Aaij *et al.* (LHCb), Phys. Rev. Lett. **122**, 222001 (2019), arXiv:1904.03947 [hep-ex].
- [3] J.-J. Wu, R. Molina, E. Oset, and B. S. Zou, Phys. Rev. Lett. **105**, 232001 (2010).
- [4] R. Chen, J. He, and X. Liu, Chin. Phys. C **41**, 103105 (2017), arXiv:1609.03235 [hep-ph].
- [5] E. Santopinto and A. Giachino, Phys. Rev. D **96**, 014014 (2017), arXiv:1604.03769 [hep-ph].
- [6] C. W. Xiao, J. Nieves, and E. Oset, Phys. Lett. B **799**, 135051 (2019), arXiv:1906.09010 [hep-ph].
- [7] R. Aaij *et al.* (LHCb), Sci. Bull. **66**, 1278 (2021), arXiv:2012.10380 [hep-ex].
- [8] T. Gershon (LHCb), (2022), arXiv:2206.15233 [hep-ex].
- [9] H.-X. Chen, W. Chen, X. Liu, and X.-H. Liu, Eur. Phys. J. C **81**, 409 (2021), arXiv:2011.01079 [hep-ph].
- [10] F.-Z. Peng, M.-J. Yan, M. Sánchez Sánchez, and M. P. Valderrama, Eur. Phys. J. C **81**, 666 (2021), arXiv:2011.01915 [hep-ph].
- [11] M.-Z. Liu, Y.-W. Pan, and L.-S. Geng, Phys. Rev. D **103**, 034003 (2021).
- [12] R. Chen, Phys. Rev. D **103**, 054007 (2021), arXiv:2011.07214 [hep-ph].
- [13] M. Karliner and J. R. Rosner, (2022), arXiv:2207.07581 [hep-ph].
- [14] J. Hofmann and M. F. M. Lutz, Nucl. Phys. A **763**, 90 (2005), arXiv:hep-ph/0507071.
- [15] V. V. Anisovich, M. A. Matveev, J. Nyiri, A. V. Sarantsev, and A. N. Semanova, Int. J. Mod. Phys. A **30**, 1550190 (2015), arXiv:1509.04898 [hep-ph].
- [16] A. Feijoo, V. K. Magas, A. Ramos, and E. Oset, Eur. Phys. J. C **76**, 446 (2016), arXiv:1512.08152 [hep-ph].
- [17] J.-X. Lu, E. Wang, J.-J. Xie, L.-S. Geng, and E. Oset, Phys. Rev. D **93**, 094009 (2016), arXiv:1601.00075 [hep-ph].
- [18] Q. Zhang, B.-R. He, and J.-L. Ping, (2020), arXiv:2006.01042 [hep-ph].
- [19] X. Hu and J. Ping, Eur. Phys. J. C **82**, 118 (2022), arXiv:2109.09972 [hep-ph].
- [20] C. W. Xiao, J. J. Wu, and B. S. Zou, Phys. Rev. D **103**, 054016 (2021), arXiv:2102.02607 [hep-ph].
- [21] J.-T. Zhu, L.-Q. Song, and J. He, Phys. Rev. D **103**, 074007 (2021), arXiv:2101.12441 [hep-ph].
- [22] X.-Z. Weng, X.-L. Chen, W.-Z. Deng, and S.-L. Zhu, Phys. Rev. D **100**, 016014 (2019), arXiv:1904.09891 [hep-ph].
- [23] X.-W. Wang and Z.-G. Wang, (2022), arXiv:2205.02530 [hep-ph].
- [24] C. Chen and E. Sparado Norella, (2022), LHCb-PAPER-2022-031 in preparation.
- [25] M.-J. Yan, F.-Z. Peng, M. S. Sánchez, and M. Pavon Valderrama, (2022), arXiv:2207.11144 [hep-ph].
- [26] F.-L. Wang and X. Liu, (2022), arXiv:2207.10493 [hep-ph].
- [27] X.-W. Wang and Z.-G. Wang, (2022), arXiv:2207.06060 [hep-ph].
- [28] J. Vijande, F. Fernandez, and A. Valcarce, J. Phys. G **31**, 481 (2005), arXiv:hep-ph/0411299.
- [29] H. Garcilazo, A. Valcarce, and F. Fernandez, Phys. Rev. C **63**, 035207 (2001).
- [30] J. Segovia, D. R. Entem, F. Fernandez, and E. Hernandez, Int. J. Mod. Phys. E **22**, 1330026 (2013), arXiv:1309.6926 [hep-ph].
- [31] P. G. Ortega, D. R. Entem, and F. Fernandez, Phys. Lett. B **718**, 1381 (2013), arXiv:1210.2633 [hep-ph].
- [32] P. G. Ortega, D. R. Entem, and F. Fernández, Phys. Lett. B **764**, 207 (2017), arXiv:1606.06148 [hep-ph].
- [33] P. G. Ortega, D. R. Entem, and F. Fernández, Phys. Lett. B **729**, 24 (2014).
- [34] D. Diakonov, Prog. Part. Nucl. Phys. **51**, 173 (2003),

- arXiv:hep-ph/0212026.
- [35] J. Segovia, A. M. Yasser, D. R. Entem, and F. Fernandez, *Phys. Rev. D* **78**, 114033 (2008).
- [36] E. Hiyama, Y. Kino, and M. Kamimura, *Prog. Part. Nucl. Phys.* **51**, 223 (2003).
- [37] R. Machleidt, in *Computational Nuclear Physics 2* (Springer, 1993) pp. 1–29.
- [38] C. G. Broyden, *Mathematics of computation* **19**, 577 (1965).
- [39] K. Azizi, Y. Sarac, and H. Sundu, *Eur. Phys. J. C* **82**, 543 (2022), arXiv:2112.15543 [hep-ph].
- [40] J. Ferretti and E. Santopinto, *JHEP* **04**, 119 (2020), arXiv:2001.01067 [hep-ph].
- [41] F.-L. Wang, R. Chen, and X. Liu, *Phys. Rev. D* **103**, 034014 (2021), arXiv:2011.14296 [hep-ph].
- [42] J. A. M. Valera, I. V. K. Magas, and A. Ramos, (2022), arXiv:2210.02792 [hep-ph].